

Underwater acoustic communication system using broadband signal with hyperbolically modulated frequency

Jan H. SCHMIDT¹, Aleksander M. SCHMIDT¹

Corresponding author: Jan H. SCHMIDT, email: jan.schmidt@pg.edu.pl

¹ Gdansk University of Technology, Faculty of Electronics, Telecommunications and Informatics, ul. Narutowicza 11/12, 80-233 Gdańsk

Abstract The implementation of reliable acoustic underwater communication in shallow waters is a scientific and engineering challenge, mainly due to the permanent occurrence of the multipath phenomenon. The article presents the concept of a transmission system using a broadband signal with hyperbolically modulated frequency (HFM) to transmit data symbols and synchronize data frames. The simulation tests were carried out in channels with Rician fading, reflecting the short- and medium-range shallow water channels. The simulation also took into account the presence of additive Gaussian noise in the channel on the functioning of the receiver. The obtained results prove the high reliability of the underwater communication system based on broadband HFM signals.

Keywords: underwater acoustic communication, shallow water, hyperbolic modulation frequency signals

1. Introduction

The development and implementation of reliable underwater acoustic communication for shallow waters are still a scientific and engineering challenge, mainly due to the unfavourable nature of the propagation conditions in the channel. There are no underwater communication systems that realise error-free data transmission in both horizontal and vertical channels using the same signals and algorithms. Compared to terrestrial radio communication, the achievable transmission rates are usually low and the variability of the propagation conditions in the channel contributes to transmission errors.

In a shallow water channel, multipath propagation has an influence on the transmitted signal due to its reflections from the boundary surfaces of the channel and objects present in the water. On the receiving side, the signals from a direct path and the paths obtained during reflections are received. The transmitted signal suffers from refraction, which is caused by significant changes in sound velocity as a function of depth. Multipath propagation and refraction produce a time dispersion in the transmitted signal. Movement of the transmitter and receiver of the communication system causes the Doppler effect, resulting in the time-domain scaling of an original broadband communication signal. This phenomenon also has a significant impact on the performance of the communication system. These unfavourable factors also occur in other communication systems, which are implemented using a different transmission medium, but it is in the water environment and with the use of acoustic waves that they are particularly enhanced. Additionally, the low speed of propagation of acoustic waves and the limited available bandwidth directly result in limiting the throughput of the hydroacoustic channel [1]. Seasonal variability in the conditions of these channels is also observed, which is an additional difficulty in defining clearly the acoustic parameters of underwater communication channels [2-4].

An efficiently operating underwater communication network must be based on a physical layer ensuring an effective and reliable acoustic communication link. In such systems, a low-rate reliable communication mode is used to initialize and re-establish a communication link, even if the transmission system is capable of operating in a higher-rate communication mode. In the event of deterioration of the propagation conditions or an increase in the noise level, the system reverts to the reliable communication mode with a low transmission rate. In addition, a reliable acoustic communication link is used in significant underwater systems that require the so-called emergency communication. For them, the transmission rate is not important, and the absolute priority is error-free data transmission.

In order to implement reliable underwater acoustic communication systems, incoherent modulations are usually used in combination with strong channel coding. They enable data transmission at a rate of hundreds of bits per second [5,6]. A significant expansion of the operating bandwidth of the system and the use of multiple hydroacoustic transducers or antennas allow for a higher transmission rate for this modulation method. The use of more transducers or antennas complicates both the hardware and the software part of the system, and thus limits its field of application. To avoid the hardware complications mentioned above, coherent modulation can be used [7-9]. However, such a modulation method requires a complex receiver due to the requirement of having significant computing power to implement the channel equalizer algorithm. Compared to non-coherent modulations, this method requires a signal with a higher signal-to-noise ratio for proper operation. Currently available modern signal processors offer sufficient computing power to implement such a system, but the problem is higher power consumption. For this modulation method, the use of more antennas operating in the same frequency band also complicates both the hardware and the software parts of the system, but allows improving the quality and transmission rate [10]. Currently, systems are mainly developed based on the technique of spread spectrum. The most popular representatives of this technique are the frequency-hopping spread spectrum (FHSS) and the direct-sequence spread spectrum (DSSS), although there are also several variations [11-15].

This article presents the implementation of reliable underwater acoustic communication for shallow waters in a configuration with one transmit and one receiving antenna (SISO). The concept of this system was presented, which is based on frequency modulated signals. The frame of transmitted data was discussed along with the preamble and postamble used. The method of data transmission assumes that there are no guard gaps between consecutively transmitted symbols. The simulation tests were carried out in channel of additive Gaussian noise and in channel with Rician fading, reflecting short and medium range shallow water channels. The article is limited to proving the correctness of the system operation in shallow waters using the selected signal, with only general consideration of the Doppler effect in a channel with Rician fading. The tests carried out showed the benefits of using this signal for the movement of the transmitter and receiver, and the results will be the subject of the next article.

2. Underwater communication system

The considered underwater communication system is designed for operation in the shallow water channel. In such a channel the phenomenon of multipath propagation occurs permanently, which causes the sent signal to reach the receiver in the form of many components of the same signal shifted in relation to each other in time. These components arrive at least two or more propagation paths (usually of different lengths). The time between the first and last components of a received multipath signal is called the multipath delay spread, and typical values for a medium range underwater communication channel are around tens of milliseconds. The mechanisms contributing to create multipath propagation depend on the geometry of the channel, the configuration of the transmitter-receiver connection (transmission range, water depth), the signal frequency, and the sound velocity profile (velocity, pressure, and salinity).

For an underwater communication system, the effect of such propagation is the occurrence of inter-symbol interference (ISI), i.e. overlapping of information symbols sent successively. The signal components of different amplitudes and phases are summed, and consequently some of them cancel each other out or add up for the same phase. The occurrence of this phenomenon is reflected in the frequency domain, where selective fading is observed at some frequencies of the used band [16-19]. Accordingly, in a channel with selective fading, the amplitude and phase of the signal at the selected frequency will constantly fluctuate, and the use of e.g. amplitude and phase modulation is exposed to strong interference, which usually makes it difficult to achieve the assumed transmission quality.

To solve the above difficulties, a broadband signal with hyperbolically modulated frequency (HFM) was used for data transmission. Signals of this type are widely used in hydrolocation systems, e.g. due to the good tolerance of the strong effects of the Doppler effect [20-22]. In the considered system, it is assumed that pulses based on the HFM signal are used with increasing (HFM-UP) and decreasing (HFM-DOWN) frequency during the pulse duration, which can be adequately written by general formulas (1) and (2).

$$s_{HFM}(t) = \exp \left[-j2\pi \frac{\ln \left(kt + \frac{1}{f_L} \right)}{k} \right], \quad (1)$$

where

$$k = \frac{f_L - f_U}{f_L f_U T_s} \text{ for HFM-UP, } k = \frac{f_U - f_L}{f_L f_U T_s} \text{ for HFM-DOWN,} \quad (2)$$

f_L is low frequency, f_U is high frequency, T_s is symbol signal duration.

The structure of the transmitted data frame consists of a preamble, a postamble, and a data block, as shown in Fig. 1. The preamble consists of two HFM pulses, each followed by a pause, the so-called guard time T_G . The first pulse (HFM-UP) increases the frequency during its duration from the lower frequency f_L to the upper frequency f_U , while the second pulse in the form of the HFM-DOWN signal decreases the frequency in time from the upper frequency f_U to the lower frequency f_L . In the postamble, HFM signals are used in reverse order than in the preamble. The transmitted data symbols are bits and are represented as follows: a logical 1 using an HFM-UP signal and a logical 0 using an HFM-DOWN signal. T_{SP} is the duration of preamble and postamble HFM signals which are equal to each other.

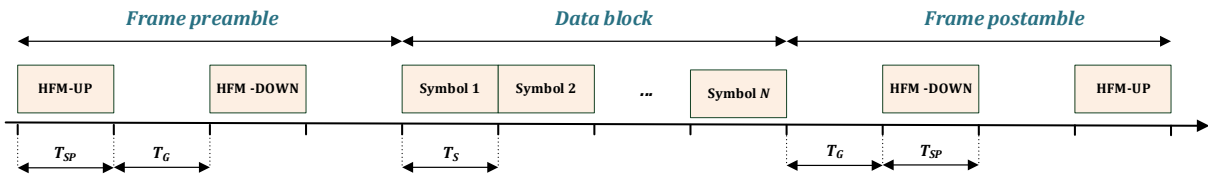


Fig. 1. Data frame structure.

2.1. Implementation of receiving part

Due to the structure of the data frame, several reception steps are performed in the receiver. During the initial reception stage, the receiver, operating in standby mode, performs real-time analysis of the incoming useful signal based on the preamble signals of the data frame. The scheme of receiving preamble, postamble and data symbol signals is shown in Fig. 2.

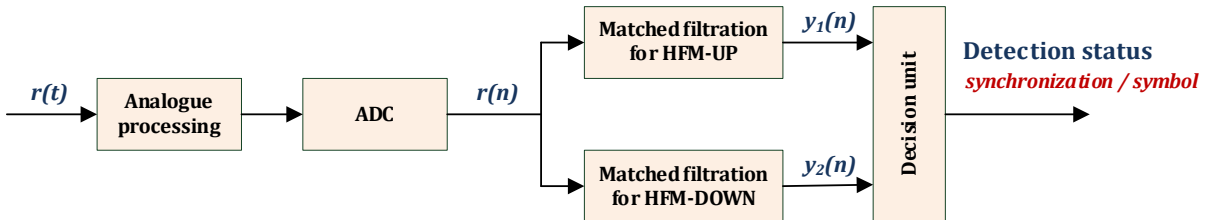


Fig. 2. The scheme of receiving preamble, postamble and data symbols signals.

As a result of the analogue processing, the analysed signal is filtered, amplified, and transformed from the band around the centre frequency to the baseband. Detection of the received HFM signals is performed by matched filtering. It is performed by determining a correlation function $y(n)$ obtained by correlating a received signal $r(n)$ and an impulse response of the matched filter $h(n)$ that is known in a system receiver according to expression (3).

$$y_{1,2}(n) = \sum_{m=0}^{M-1} h(m)r(n - m), \quad (3)$$

The correlation functions performed in the time domain are interpreted as signal compression and are performed in parallel for both the HFM-UP and HFM-DOWN transmitted pattern signals. For example, for the established times $T_{SP}=64$ ms and $T_G=64$ ms, where the frame preamble, postamble and data signal $r(t)$ described by formulas (1) and (2) and the determined correlation functions for the received signal and the pattern signals of HFM-UP and HFM-DOWN, are presented in Fig. 3. The advantage of using matched filtering is to improve the input signal-to-noise ratio of the receiver (SNR) BT times at its output, where B is the signal bandwidth and T is its duration, according to equation (4). SNR_y is the signal-to-noise ratio of the

output signal. For the applied broadband signal, this improvement is achieved by increasing the value of B or T . Increasing the bandwidth of the signal increases the resolution of the correlation functions obtained.

$$\text{SNR}_y = BT \cdot \text{SNR}. \quad (4)$$

In the initial reception step, in addition to detecting the signal arrival, synchronization of the transmitter and receiver is also performed, and thus a time relationship is established between the individual signals in the data frame. An additional use of the preamble is the estimation of the channel parameters based on the obtained *channel impulse responses* (CIR), which will be used during the proper reception of the data block.

In the preamble of the data frame, two pulses with a hyperbolically modulated frequency are used, but with different monotonicity of the varying frequency of the signal over time. This allows for unambiguous determination of the delay assumed in the transmitter between them and determination of the Doppler shift. The property that concerns the influence of the Doppler effect on the obtained correlation functions for the applied signals is helpful here. The correlation functions for the HFM-UP and HFM-DOWN signals are time-shifted against the reference function for the same deviation, that is, the autocorrelation function, for cases where the transmitter approaches the receiver or moves away.

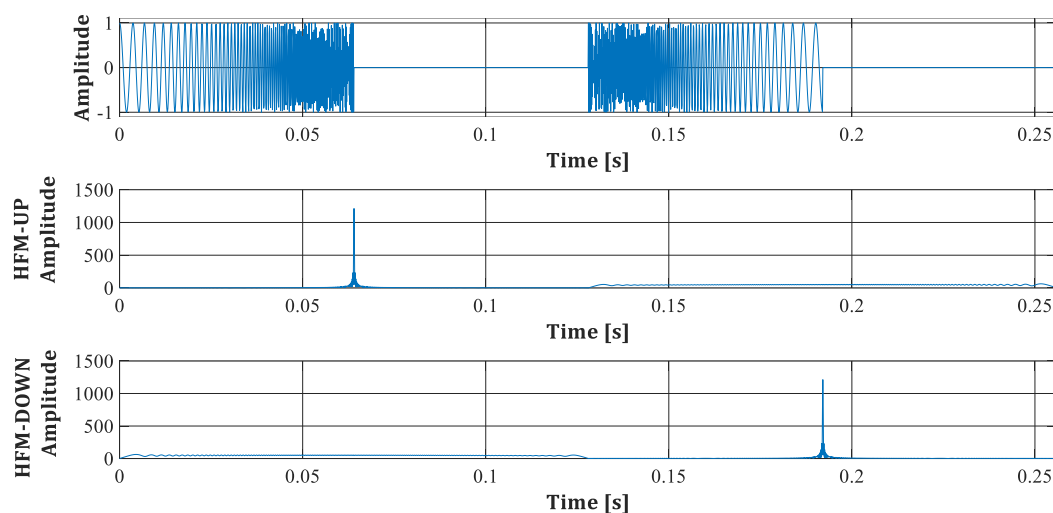


Fig. 3. The frame preamble signal and the determined correlation functions for the received signal with the pattern HFM-UP and HFM-DOWN signals ($T_{sp}=64$ ms, $T_G=64$ ms).

Almost analogously to the preamble, a packet of data transmitted over a communication channel is received. As mentioned previously, the transmitted data symbols are encoded bits as follows: logic 1 as the HFM-UP signal and logic 0 using the HFM-DOWN signal. After the data block has been synchronized with the preamble of the frame, subsequent data symbols are received according to the data reception scheme of Fig. 2.

The good tolerance of the strong Doppler effects on the HFM signal, mentioned at the beginning of the chapter, consists in much smaller changes in the maximum value of the correlation function than for the widely used linear frequency modulation (LFM) signal. Therefore, the conditions for detecting signals with hyperbolic frequency modulation are almost independent of the speed of the observed targets [21,22].

3. Simulation tests

To carry out the tests, it was assumed that the total operating band of the data transmission system was $B=5$ kHz. The bandwidth signal around the centre frequency $f_0=30$ kHz is transmitted through the acoustic underwater channel, then it is sampled at the receiver at 200 kHz and after conversion to the baseband its sampling frequency is $f_s=10$ kHz.

Fig. 4 presents the correlation functions obtained for the HFM-UP pulse transmitted by the communication channel model with additive Gaussian noise in the case where the SNR is -10dB and 20dB.

Each of the transmitted pulses comprises a single HFM-UP signal period, a duration T_s of 64 ms, and a band B of 5 kHz, a Doppler shift of 0 Hz. There was no multipath propagation in the communication channel.

When receiving a signal in the presence of additive Gaussian noise, the signal-to-noise ratio is proportional to the energy of the received signal and inversely proportional to the noise power spectral density. The narrow main beam of the correlation function and the low level of side lobes are the advantages of using a broadband signal. The correlation functions determined for various Gaussian noise values showed compliance with dependence (4).

Based on Fig. 4 it can be clearly assessed that the narrow main beam of the correlation function was obtained. The width of this beam corresponds to the beam of the main autocorrelation function established between its first zeros equal to $2/B$, therefore for $B=5$ kHz it is $\Delta t = 0.4$ ms. Thus, an improvement in the temporal resolution of the correlation function was achieved along with the broadening of the signal band B . The maximum value of the correlation function is proportional to the signal duration and more precisely to the number of samples per time. The repeatability of the obtained maximum values of the correlation function is greater, the higher the SNR of the analysed signal. The differences also result from the applied bandwidth of the B signal: when the band is wider, the smaller the differences. Extending the signal duration allows one to reduce the noise influence on the obtained value of the correlation function.

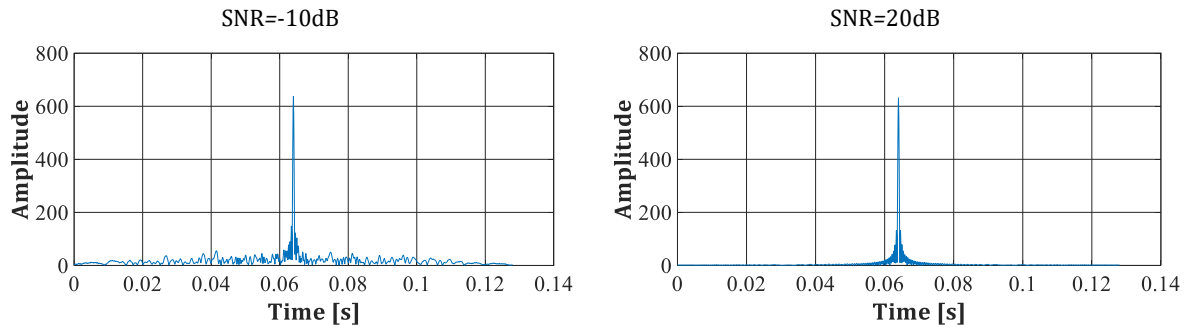


Fig. 4. The correlation functions of the received signal and the transmitted pattern HFM-UP signal, for the case of transmission in a channel with different levels of additive Gaussian noise of a signal with a duration of $T_s=64$ ms.

For SNR = -10dB, the maximum values of the correlation function take the following values: 40.8 for $T_s=4$ ms, 157.2 for $T_s=16$ ms and 603.4 for $T_s=64$ ms. In turn, for SNR = 20 dB these values are: 39.2 for $T_s=4$ ms, 152.4 for $T_s=16$ ms and 606.9 for $T_s=64$ ms. Despite the large differences between the SNRs, the obtained values of the correlation function for the same durations are comparable.

The considered underwater acoustic communication system is designed to work in a shallow water channel, i.e. a channel in which multipath propagation permanently occurs, and the transmitted signal is subject to fading. This channel can be presented as a linear filter whose complex lowpass impulse response $h(\tau, t)$ is the sum of the impulse responses corresponding to all propagation paths of n , where each of these paths is described by the corresponding amplitude $a_n(t)$, phase $\varphi_n(t)$ and delay $\tau_n(t)$. Delay τ concerns only paths obtained during reflections and the value of these paths depends on their geometry. The number $N(t)$ is the maximum number of propagation paths during transmission, depending on t . This filter is described as (5) and relates to a nonstationary underwater channel, in which the received signal parameters (amplitude, phase, and delay) are functions of time t . In this approach, it is assumed that the individual components of the incoming signal are mutually uncorrelated.

$$h(\tau, t) = \sum_{n=1}^{N(t)} a_n(t) e^{-j\varphi_n(t)} \delta(\tau - \tau_n(t)), \quad (5)$$

where $\varphi_n(t) = 2\pi f_c \tau_n(t)$ and f_c is the nominal carrier frequency.

For simulation tests, the configuration of the communication channel assumes the occurrence of a direct propagation path (LOS, *line-of-sight*). Therefore, the Rician fading channel model has been used, which is used when the direct and the reflected signals are received. The dominant direct component is usually associated with the direct propagation path with the highest power. The channel model with Rician fading is suitable for the simulation of a short- and medium-range transmission channel [23].

When the envelope of the impulse response $R=|h(\tau,t)|$ has a real component R_r and imaginary component R_i , which are independent random variables with Gaussian distributions $N(\mu_r, \sigma^2)$ and $N(\mu_i, \sigma^2)$ with respective mean values μ_r and μ_i , and variance σ^2 , where $R = \sqrt{R_r^2 + R_i^2}$, the envelope of the received signal has the Rician distribution with the probability density function described as (6):

$$p_{Rice}(r) = \frac{r}{\sigma^2} e^{-\frac{(r^2+s^2)}{2\sigma^2}} I_0\left(\frac{rs}{\sigma^2}\right) \text{ for } r \geq 0, \quad (6)$$

hence, the amplitude of the direct path signal has the form (7):

$$s = \sqrt{\mu_r^2 + \mu_i^2}. \quad (7)$$

I_0 is the modified Bessel function of the first kind and of zero order. An important parameter of the Rician model is the K factor, which determines the ratio of the direct path component (dominant component) to the power in all the other components. It can be expressed as (8):

$$K = \frac{s^2}{2\sigma^2}. \quad (8)$$

The phase $\varphi_n(t)$ of received signal is uniformly distributed in the interval $[0, 2\pi]$.

To estimate the performance of the underwater communication system with the HFM signal, simulation tests were carried out in a channel with frequency-selective fading, in which there is a multipath effect [23,24]. In the frequency-selective fading case, the received signal consists of multiple copies of transmitted signal, attenuated and delayed in time. The path parameters for a specific transmitter-receiver configuration have been predetermined, i.e. delays of multipath components and their average path gain, where average path gain is normalized to 0 dB. The first four dominant rays were taken into account. The parameters are supposed to reflect the transmission between the transmitter and the receiver, which are 300m away, in a 20m deep water reservoir, with the same transmitter and receiver depth of 10 m. The parameters of multi-path paths were determined for the acoustic wave propagation speed $c = 1475$ m/s and are as follows - for 1st path (direct): delay 0 ms, average path gain 0 dB; 2nd path: 4.74 ms, -3 dB; 3rd path: 7.45 ms, -4.6 dB; 4th path: 11.5 ms, -6 dB. Therefore, the multipath delay spread T_m , which specifies the time between the first component of the received signal and the last component of the received multipath signal, is 11.5 ms. This is a typical value for a short- and medium-range underwater communication channel.

The determined parameters were used to carry out a series of transmission tests of the symbol sequence of binary data 1 and 0 encoded with HFM-UP and HFM-DOWN signals, respectively. There were no guard gaps between the transmitted symbols. Signals with different T_s durations were sent by channel model with Rician fading and in the presence of additive Gaussian noise, and the obtained results are presented in the Tab. 1.

Tab. 1. The determined Bit Error Rate (BER) values for different values of T_s and SNR ($K=3$ dB).

		SNR				
		-20 dB	-10 dB	0 dB	10 dB	20 dB
T_s	4 ms (BT=20)	0.43	0.14	0.12	0.11	0.12
	8 ms (BT=40)	0.32	0.027	0.021	0.021	0.021
	16 ms (BT=80)	0.12	<10 ⁻⁶	<10 ⁻⁶	<10 ⁻⁶	<10 ⁻⁶
	64 ms (BT=320)	0.00014	<10 ⁻⁶	<10 ⁻⁶	<10 ⁻⁶	<10 ⁻⁶

The obtained results indicate that the transmission is error-free or takes place with single errors when the condition $T_s > T_m$ is met. Cases where this condition is not met can be clearly seen for $T_s=4$ ms and $T_s=8$ ms, for which the obtained BER is high and does not depend on the SNR.

In turn, properly selected signal duration of symbol T_s , and hence the product BT , determines the possibility of working with low SNR. And so, for $T_s=64$ ms, which gives a high product of $BT=320$, almost error-free data transmission is possible at SNR= -20 dB. The remaining signal durations of symbol $T_s=4$ ms, 8ms and 16ms yield values of product BT that are too small for this SNR value. In summary, the BER results prove the high reliability of the underwater communication system based on broadband HFM signals.

In Fig. 5 and Fig. 6, the determined correlation functions for the received signal of the transmitted sequence of binary symbols 111001100 in the channel with Rician fading are shown, for symbol signal duration $T_s=16$ ms, Doppler shift f_d of 0 Hz at SNR = -10 dB and SNR = 20 dB. For this type of channel, it is possible to distinguish the direct path component and successively arriving multipath components even when the Doppler shift f_d has a relatively large value, e.g. 100 Hz. No significant influence of the Doppler effect on the deterioration of the efficiency of the communication system was observed.

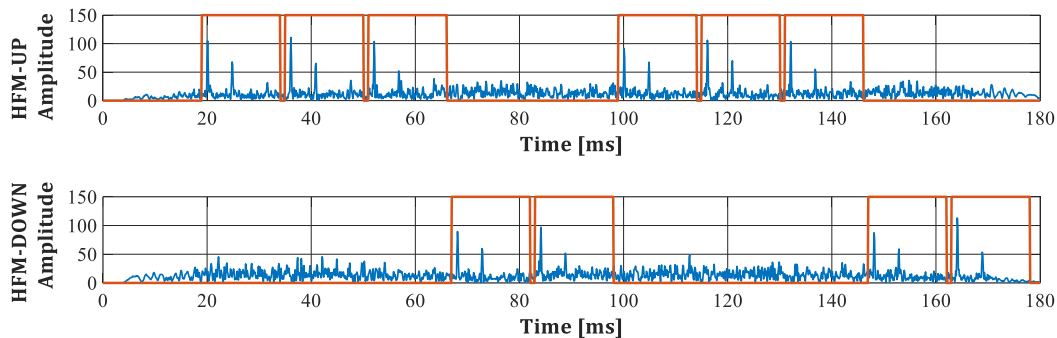


Fig. 5. The correlation functions of the received signal and the transmitted patterns HFM-UP and HFM-DOWN signal, for transmission of binary symbol sequences 111001100 over the channel with Rician fading at SNR = -10 dB ($T_s=16$ ms, $f_d=0$ Hz).

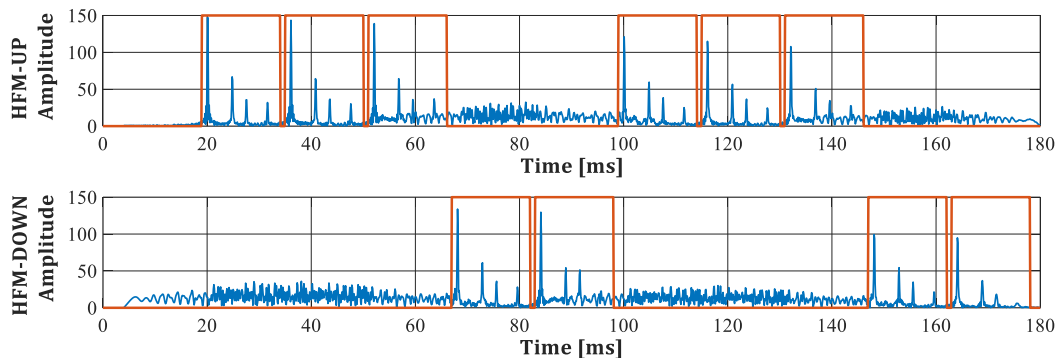


Fig. 6. The correlation functions of the received signal and the transmitted patterns HFM-UP and HFM-DOWN signal, for transmission of binary symbol sequences 111001100 over the channel with Rician fading at SNR = 20 dB ($T_s=16$ ms, $f_d=0$ Hz).

The transmission rates of the symbols are low and depend on the duration of the symbols T_s . For $T_s=16$ ms it is 62.5 bps and for $T_s=64$ ms it is about 15.6 bps. In the considered system, reliable data transmission without the need for adaptive reception techniques is the priority, not the transmission rate.

4. Conclusions

Simulation tests were carried out for the concept of an underwater communication system based on broadband HFM signals presented in the article. The obtained results prove the high reliability of the system. The system shows high resistance to additive Gaussian noise and the influence of the Doppler effect. Properly selected durations of the HFM signals that represent logical 1 and 0 data symbols ensure reliable data transmission and allow the system to operate in covert communication mode. The concept of the underwater acoustic communication system presented here was created to be used to implement a low-power transceiver operating on the basis of a single-chip processor.

Additional information

The authors declare no competing financial interests.

References

1. X. Lurton. An Introduction to Underwater Acoustics: Principles and Applications. Springer, 2010.
2. G. Grelowska. Study of Seasonal Acoustic Properties of Sea Water in Selected Waters of the Southern Baltic. Polish Maritime Research, 23:25–30, 2016. DOI: 10.1515/pomr-2016-0004.
3. B. Katsnelson, V. Petnikov, J. Lynch. Fundamentals of Shallow Water Acoustics. Springer, 2012.
4. P.C. Etter. Underwater Acoustic Modeling and Simulation. CRC Press, 2018.
5. H.S. Dol, P. Casari, T. van der Zwan, R. Otnes. Software-Defined Underwater Acoustic Modems: Historical Review and the NILUS Approach. IEEE Journal of Oceanic Engineering, 42:722–737, 2017.
6. D. Garrod. Applications of the MFSK Acoustic Communications System. OCEANS 81, 1981. DOI: 10.1109/OCEANS.1981.1151697.
7. M. Stojanovic, J.A. Catipovic, J.G. Proakis. Phase-coherent digital communications for underwater acoustic channels. IEEE J. Ocean. Eng., 19:100–111, 1994. DOI: 10.1109/48.289455.
8. J.H. Schmidt, A.M. Schmidt, I. Kochanska. Performance of Coherent Modulation Scheme Used in Acoustic Underwater Communication System. Vibrations in Physical Systems, 30(1):2019135, 2019.
9. I. Kochanska, J.H. Schmidt, J. Marszal. Shallow water experiment of OFDM underwater acoustic communications. Archives of Acoustics, 45(1): 11–18, 2020.
10. J.H. Schmidt, A.M. Schmidt, I. Kochanska. Multiple-Input Multiple-Output Technique for Underwater Acoustic Communication System. In Proceedings of 2018 Joint Conference Acoustics, Ustka, Poland, 11–14 September 2018. DOI:10.1109/ACOUSTICS.2018.8502439.
11. J.G. Proakis. Digital Communication. McGrawHill, New York, 2000.
12. Don Torrieri. Principles of Spread-Spectrum Communication Systems. Springer, 2018.
13. J.H. Schmidt. Using Fast Frequency Hopping Technique to Improve Reliability of Underwater Communication System. Applied Sciences, 10(3):1172, 2020. DOI: 10.3390/app10031172.
14. I. Kochanska, R. Salamon, J.H. Schmidt, A.M. Schmidt. Study of the Performance of DSSS UAC System Depending on the System Bandwidth and the Spreading Sequence. Sensors, 21(7):2484, 2021. <https://doi.org/10.3390/s21072484>.
15. I. Kochanska, J.H. Schmidt. Simulation of Direct-Sequence Spread Spectrum Data Transmission System for Reliable Underwater Acoustic Communications. Vibrations in Physical Systems, 30(1):2019108, 2019.
16. M.K. Simon, M-S. Alouini. Digital Communication over Fading Channels. Wiley-IEEE Press, 2005.
17. A.F. Molisch Wireless Communications. Wiley-IEEE Press, 2010.
18. B. Sklar. Rayleigh fading channels in mobile digital communication systems. Part I. Characterization. IEEE Communications Magazine, 35(7):90-100, 1997.
19. B. Sklar. Rayleigh fading channels in mobile digital communication systems. Part II: Mitigation. IEEE Communications Magazine, 35(9):148-155, 1997.
20. J. Marszal. Experimental Study of Silent Sonar. Archives of Acoustics, 39(1), 2015. DOI: 10.2478/aoa-2014-0011.
21. J.J. Kroszczyński. Pulse compression by means of linear-period modulation. Proc. IEEE, 57(7):1260–1266, 1969.
22. J. Yang, T.K. Sarkar. Doppler-invariant property of hyperbolic frequency modulated waveform. Microwave and optical technology letters, 48(8):1174–1179, 2006.
23. J.G. Proakis, M. Salehi, G. Bauch. Contemporary Communication Systems using Matlab (Third Ed.). Prentice Hall, Cengage Learning 2013.
24. I. Kochanska, J.H. Schmidt. Estimation of Coherence Bandwidth for Underwater Acoustic Communication Channel. In Proceedings of 2018 Joint Conference Acoustics, Ustka, Poland, 11–14 September 2018. DOI: 10.1109/ACOUSTICS.2018.8502331.

© 2021 by the Authors. Licensee Poznan University of Technology (Poznan, Poland). This article is an open access article distributed under the terms and conditions of the Creative Commons Attribution (CC BY) license (<http://creativecommons.org/licenses/by/4.0/>).